Stochastic effects in the representation of stratocumulus-topped mixed layers

Bjorn Stevens, Yunyan Zhang and Michael Ghil

Department of Atmospheric and Oceanic Sciences
and Institute for Geophysics and Planetary Physics
University of California at Los Angeles
Los Angeles, CA 90095-1565, USA

1. Introduction

Stratocumulus clouds are an integral component of the climate system. They affect both its mean state and variability, and are central to many questions related to climate change. They are also very difficult to represent with fidelity in modern forecast systems and climate models. Their importance is associated with what one may call long-term climatic robustness, which is in marked contrast to the physical sensitivity they exhibit at any particular time, and which is one of the main reasons they prove so difficult to represent.

Some of these points are evident in the panels of Fig. 1. On the upper left we show a snapshot of stratocumulus in the northeast Pacific from the GOES-10 satellite. Striking about this figure is the extent to which a variety of aspects of the flow imprint themselves on the cloud field. A ring of vortices appears near the channel islands off Pt. Conception and a trailing vortex streaks downstream of Guadalupe. Even the apparently cloud-free region west of 120W is probably covered by a very thin veil of clouds. Two ship plumes are also evident as one moves to the northwest from the center point at 30N and 120W. Further evidence of this sensitivity is the extent to which the cloud field respects the coastal boundary, and local coastal flows such as those southeast of Sebastián Vizcaino Bay on the bottom right of the figure.

In the upper right panel we show a region of more evidently cellular stratocumulus as seen by MODIS. Here both open and closed cells are illustrated, with closed cells (the bright areas) being the predominant form of stratocumulus organization (Agee, 1984; Atkinson and Zhang, 1996). Recent work suggests that pockets of open cells (the dark areas) such as shown in this figure might be associated with the development of precipitation (Stevens et al., 2005b). The possibility that precipitation, and by inference aerosol effects, may so markedly affect cloud evolution motivates the interest of the broader scientific community in this cloud form. Stratocumulus cloud systems are thus quite sensitive to the large-scale conditions, on the one hand, and display a great degree of internal variability on various time and space scales, on the other. This may explain why their representation in modern forecast systems proves so challenging.

The sensitivity of stratocumulus decks results from the balance of disparate physical processes (cloud microphysical processes, radiation, and fine-scale turbulence) operating on the convective time scale (order 10 min) at an interface with very fine vertical scales (cf. conceptual diagram at bottom of Fig. 1). Properly coupling processes which are distinct from the perspective of the host model (i.e., radiation, cloud and turbulent processes) has proven to be an engineering challenge, and accounting for the structure of the interface, where temperatures can change on scales of 10 m by 10 K, and mixing ratios can fall off to near zero, only adds to the challenge.

In this paper we investigate the representation of stratocumulus clouds by the Integrated Forecast System (IFS) of the ECMWF, as well as its representation of the large-scale environment. We show that the IFS and the

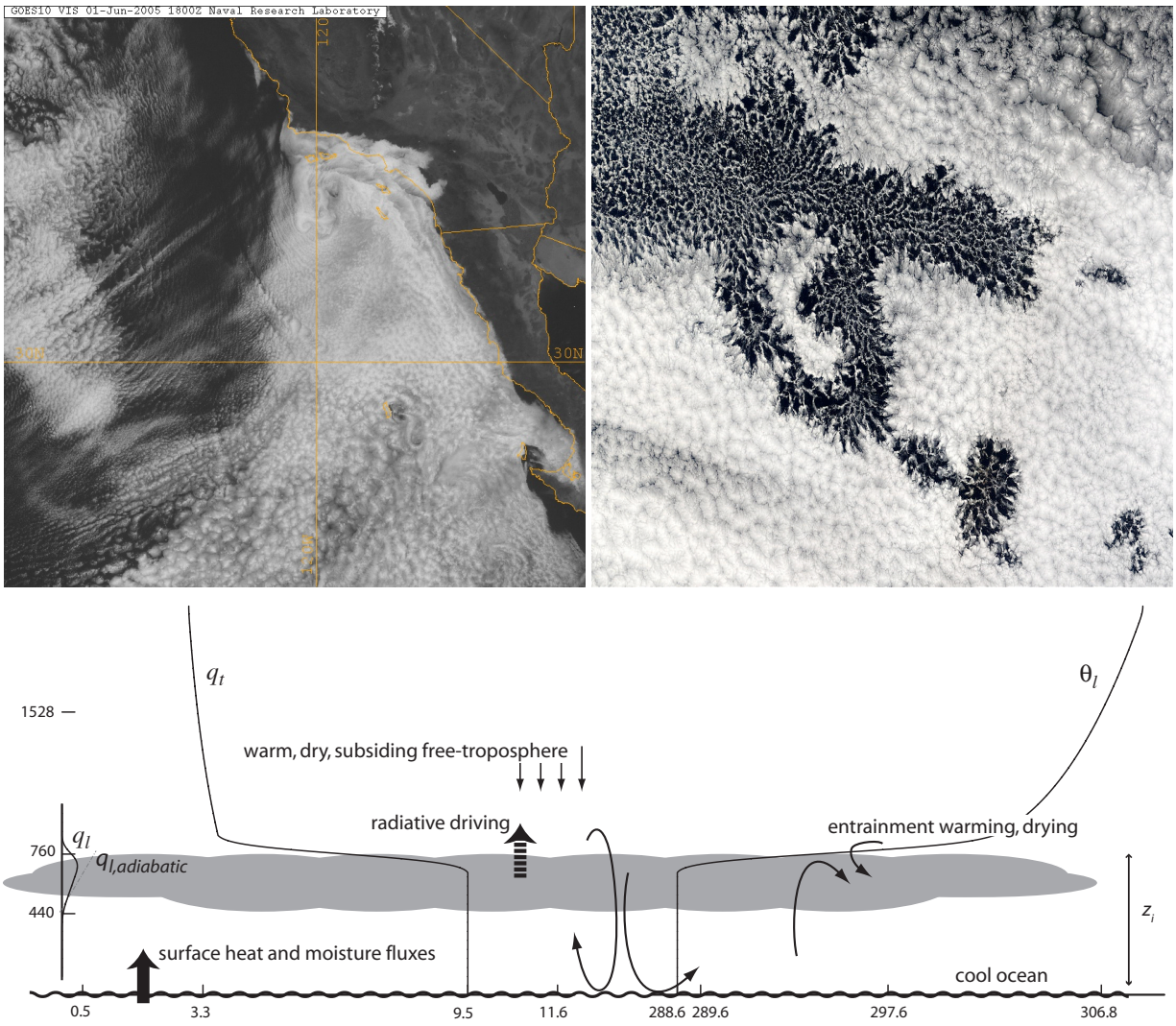

Figure 1: Left upper panel: GOES-10 visible imagery of the northeast Paci c stratocumulus topped boundary layer, near 120W and 30N. Right upper panel: MODIS imagery of the Southeast Paci c stratocumulus regions showing open (relatively dark) and closed (relatively bright) cells thought to be associated with precipitation development. Lower panel: mean thermodynamic structure superimposed on a conceptual cartoon of the physical processes that govern the behavior of non-precipitating stratocumulus.

40-year reanalysis of meteorological data by the ECMWF (ERA40) represent well the large-scale conditions in the remote marine environment occupied by stratocumulus, but that the boundary layer structure is less well represented. We then develop a single-column, highly idealized model, which we force with ERA40 climatological forcing to investigate the misrepresentation of the stratocumulus-topped boundary layer by the IFS, and the extent to which it may be associated with unresolved processes that can be represented stochastically.

To evaluate the representation of the stratocumulus-topped boundary layer, and of the larger-scale environment, by the IFS we use data collected as part of the DYCOMS-II field program (Stevens et al., 2003). DYCOMS-II consisted of ten (mostly nocturnal) research flights in the heart of the stratocumulus region of the North Pacific; most flights were centered near 120W and 30N. Because operating times and flight areas were restricted during DYCOMS-II, there was relatively little chance to target flights to specific flow features; as a result the flight data provide a relatively unbiased sampling of the lower troposphere near 120W and 30N during the period of flight operations in July 2001. Moreover, during the period of flight operations, IFS and NCEP's Global Forecast System (GFS) data sets were made available to the investigators, thus providing an opportunity to assess the representation of the stratocumulus-topped boundary layer by the IFS and GFS. The IFS data were provided in the Diagnostics sur Domaines Horizontaux (DDH) format, which contains model level fields averaged over a specific geographic region, in this case the DYCOMS-II flight area, or at a single model node.

Some results from this analysis are shown in Fig. 2. This figure is adapted from Stevens et al. (2005a), who present a more detailed evaluation of the forecast systems and various satellite remote sensors over the DYCOMS-II region. In this figure, ERA data are presented by the larger, grey, open and closed circles. Flight data are shown by black circles, and various satellite products are marked as indicated in the legend at the top of the diagram.

The figure contains a considerable amount of information, from which we only extract two essential points:

- The large-scale state of the free troposphere is well represented by ERA40. This is evident in the good agreement between ERA40 boundary layer winds and divergence with estimates by both *in situ* probes and remote sensors, as well as good representation of column water path (of which less than half is associated with the boundary layer), and free tropospheric temperatures.
- The greatest discrepancies between ERA40 and the data is in the representation of the boundary layer structure itself: the boundary layer is too shallow, winds are insufficiently zonal, and cloud water is significantly under-represented.

Such deficiencies in the representation of the stratocumulus-topped boundary layer are characteristic of large-scale models. If anything the representation by the ERA40 (and the IFS, not shown) is much better than many other contemporary models. Many meso- or regional-scale models run over the region of field operations struggle to maintain a cloud layer at all, a difficulty shared by the GFS model maintained by NCEP. This is evident in Fig. 3 where we show the mean July 2001 structure of the cloud-topped boundary layer as represented by the IFS, the GFS, and the ERA40. For reference the mean profile as deduced from flight data is given by the bottom panel of Fig. 1. Here we note that overall the IFS tends to maintain a boundary-layer top which is much more diffuse, and a boundary layer thermodynamic structure which is significantly more stratified than observed (e.g., its gradients in boundary layer specific humidity tend to be larger than observed) and have much too little liquid water; the 3 K warm bias in the GFS is an even more serious deficiency.

From this analysis (see Stevens et al., 2005a, for futher details), we conclude that climatological biases in the representation of stratocumulus by the ERA40 and the IFS are principally due to deficiencies in the parameterization of processes in the cloud-topped boundary layer, and not in the large-scale state which acts as boundary conditions for these parameterizations. In the remainder of this paper, we explore the hypothesis that the deficiencies in the parameterizations can be remedied by accounting for parameter uncertainty, and unresolved fast

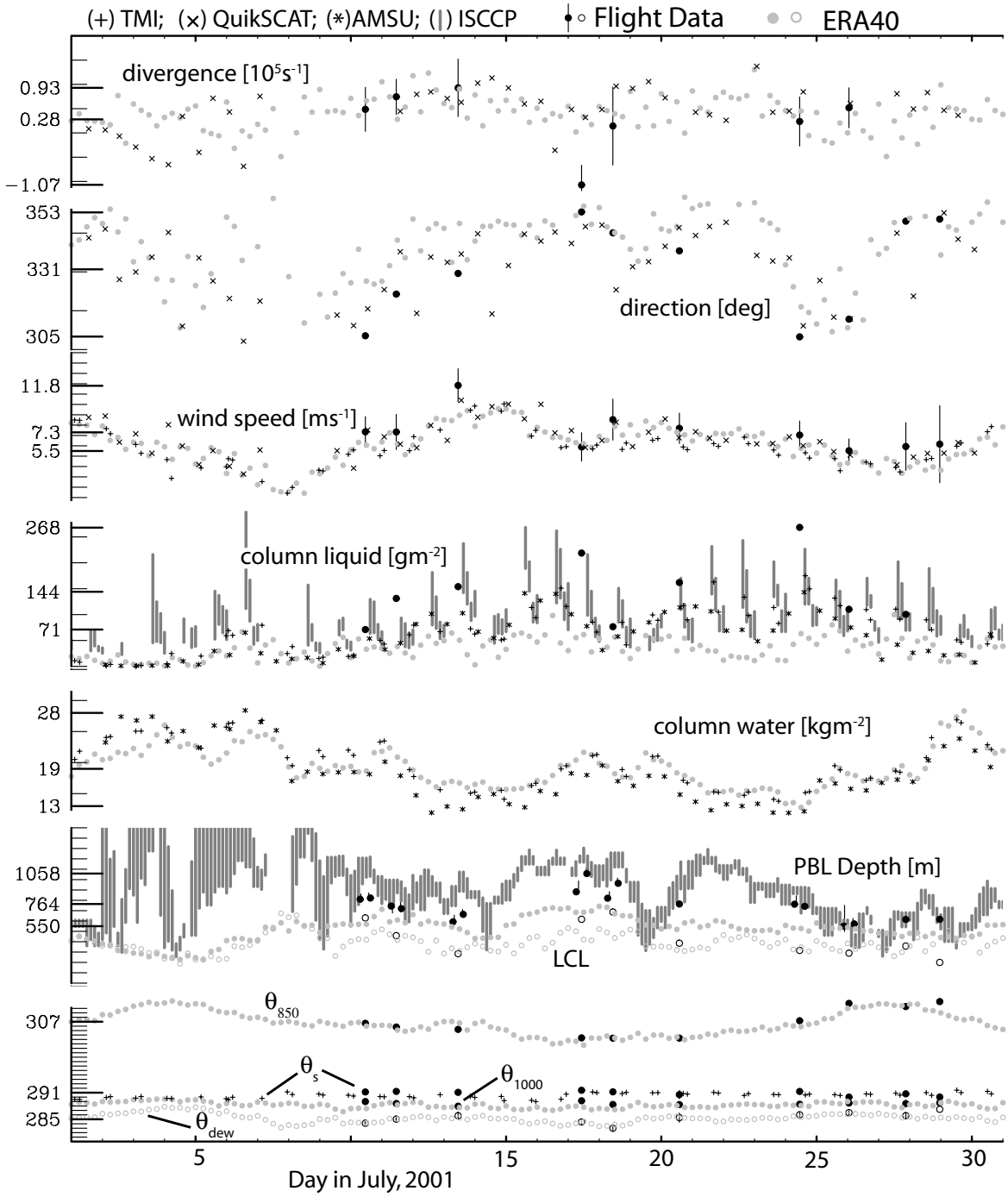

Figure 2: Synthesis of ight and routine data over the DYCOMS-II study area for July 2001. Estimates of variability accompany the ight data, open circles in bottom panel denote θ_{dew}, and open circles in second panel from bottom denote Lifting Condensation Level (LCL). For reasons of clarity the NCEP data are not included in this plot. Vertical axes labels minimum, mean and maximum of ight data.[After Stevens et al. (2005a).]

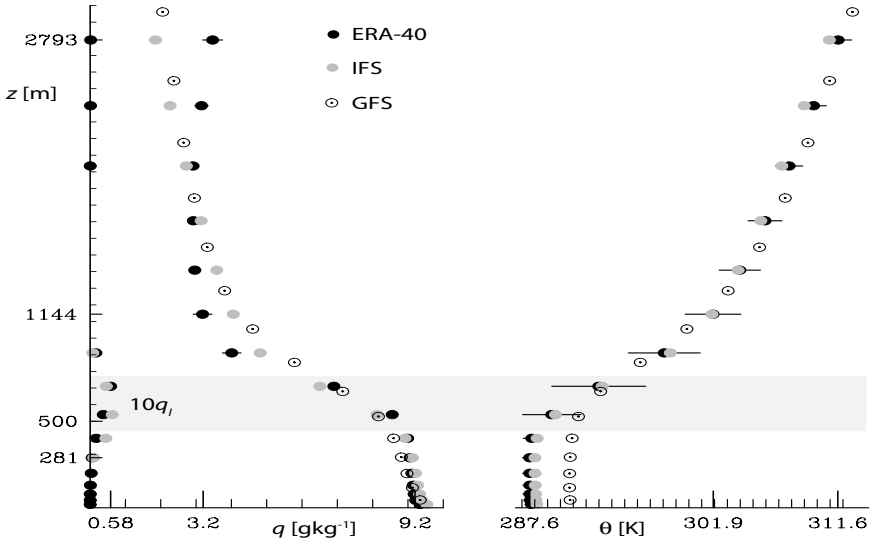

Figure 3: Mean pro le for July 10–20, 2001, for ERA-40, GFS and IFS 0000–2400 UTC forecasts. For guidance the position of the observed cloud layer is indicated by the shading.

processes, using stochastic methods. We do so by using a highly idealized representation for the IFS boundary layer model and evaluate its agreement with the full IFS simulation.

2. The deterministic mixed-layer model

To represent the boundary layer given large-scale forcing, we use the single-column mixed-layer model of Lilly (1968); see also Stevens (2005). For the stratocumulus layer with fixed advective forcing this amounts to solving three weakly nonlinear ordinary differential equations (ODEs) representing the conservation of mass, enthalpy, and moisture respectively. The three ODEs govern the depth of the boundary layer h, the liquid water static energy $s = c_p T + gz - q_l z$, and the total water specific humidity q:

$$\begin{aligned} d_t h &= E - \mathscr{D} h - \widehat{\mathbf{u}} \cdot \nabla h \ , \\ d_t \widehat{s} &= E(s_+ - \widehat{s}) + V(s_0 - \widehat{s}) - \Delta F - \widehat{\mathbf{u}} \cdot \nabla \widehat{s} \ , \\ d_t \widehat{q} &= E(q_+ - \widehat{q}) + V(q_0 - \widehat{q}) - \widehat{\mathbf{u}} \cdot \nabla \widehat{q} \ ; \end{aligned} \tag{1}$$

the carat indicates a value averaged over the depth of the boundary layer, subscript 0 denotes a surface value, and subscript "+" denotes values valid just above the boundary layer.

The radiative driving of the system is given by ΔF, $\mathscr{D}$ denotes the divergence $\nabla \cdot \widehat{\mathbf{u}}$, and V is a surface exchange velocity. Here $\mathbf{u}$ and ∇ both refer to the horizontal plane. To the extent to which the layer is well mixed, so that $\widehat{s}$ and $\widehat{q}$ are characteristic of their surface-layer values, V is reasonably well determined by surface layer similarity as proportional to the surface wind speed, such that $V = 0.001\|\widehat{\mathbf{u}}\|$. Precipitation is not considered at this point. The principal closure assumption lies in the specification of the entrainment velocity E. Determining E in this context has been the subject of extensive research over the past decades, with many past proposals reviewed by Stevens (2002).

For our investigations, E recognizes two sources of entrainment: buoyancy-driven turbulence, based on a recent

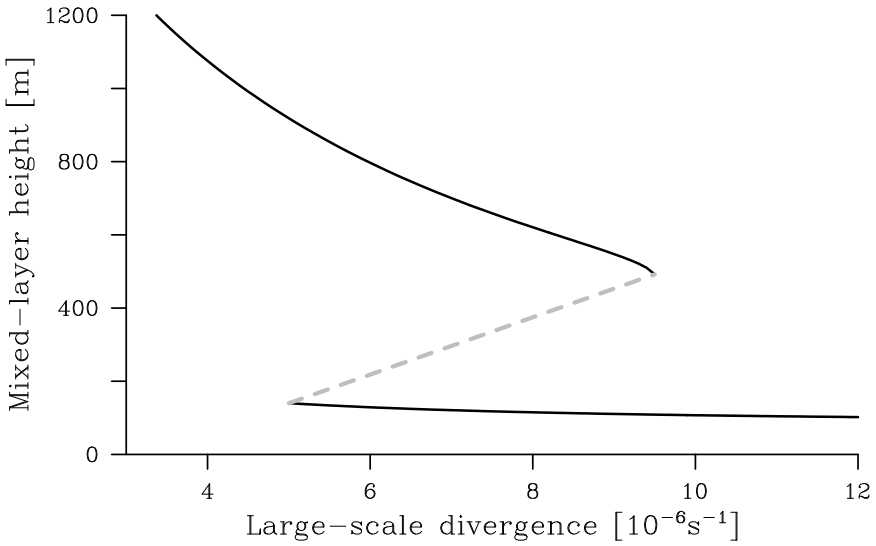

Figure 4: Illustration of the multiple equilibria of the mixed-layer model as a function of the large-scale divergence $\mathscr{D}$.

proposal by Lewellen and Lewellen (1998), and shear-driven turbulence. The latter addition is critical to an interesting property of the model, namely its production of multiple equilibria Randall and Suarez (1984).

In Fig. 4 equilibrium boundary layer heights are shown as a function of the large-scale divergence. The figure illustrates the fact that, in a parameter range characteristic of the main stratocumulus regions, the model supports both shallow and deep solutions. The deep solutions correspond to cool, moist stratocumulus-topped boundary layers whose entrainment is maintained by buoyant convection driven by radiative cooling at cloud top. The shallow equilibria correspond to warm, dry, clear boundary layers for which shear production is the primary source of turbulence, and hence entrainment.

This bimodality can play an important role in the effects of stochastic perturbations on the large-scale organization of the cloud deck. To understand this, it suffices to recall the role played by such S-shaped bifurcation curves in energy balance climate models (North et al., 1981; Ghil and Childress, 1987), large-scale atmospheric dynamics (Charney and DeVore, 1979; Koo and Ghil, 2002), and radiative-convective models (Li et al., 1997; Rennó, 1997).

Equilibria of system (1) forced by the mean conditions observed during DYCOMS-II are presented in Fig. 5. Also on this figure are plotted the results from the IFS. We note that the equilibria of (1) are plausible representations of the boundary layer state. When advection is included they tend to lie somewhat closer to the observed state than does the IFS, i.e., the observations lie closer to the model solution at $\mathscr{D} = 4 \times 10^{-6}$ than they do to the ERA40 result, except for the humidity field, where the difference is negligible. The tendency of the steady states of (1) to over-predict the cloud liquid-water path reflects the adiabaticity assumption for liquid water. If we had used the DYCOMS-II empirical result for cloud-water lapse rates with the mixed-layer model prediction of cloud base and cloud top, the correspondence between the mixed-layer solutions and the data in Fig. 5 would have been even closer. That said, the point of this figure is not to establish the single-column model (1) as clearly superior to the IFS parameterization; indeed, as the figure shows, the fitness of our model's solutions depends critically on the inclusion of advective processes. We merely wish to establish (1) as a plausible representation of the IFS's boundary layer physics.

The use of the mixed-layer model (1) to capture the IFS physics has three main advantages: (i) it is much simpler than a single-column representation of the full IFS physics; (ii) as a system of ODEs it is grid independent, and

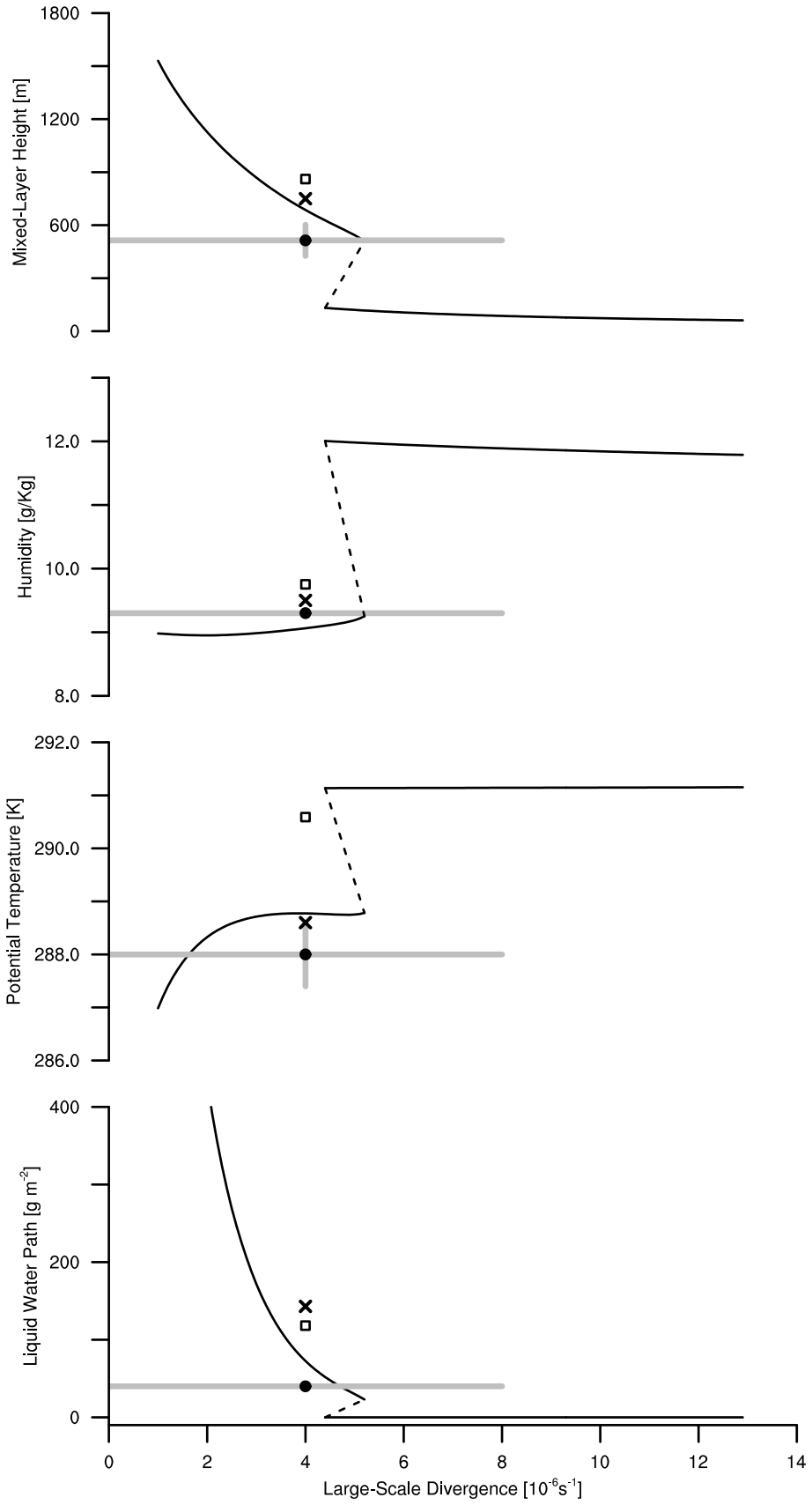

Figure 5: Steady-state solutions of (1) as a function of the large-scale divergence $\mathcal{D}$, with other forcing as given by ERA40. The observed state is given by the 'x'; ERA40 results are given by the lled dots, the abscissa of the error bar determining the standard deviation in forcing. The open squares denote equilibrium solutions at the mean forcing with advective terms neglected.

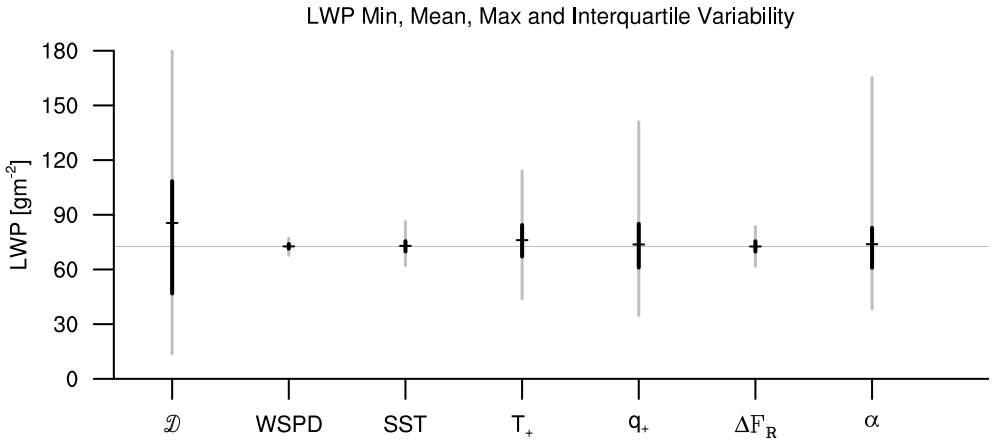

Figure 6: Minimum, maximum, mean and interquartile variability of liquid water path (LWP) as a function of which large-scale variable is allowed to vary randomly. The horizontal grey line is the mixed-layer mean LWP state subject to mean forcing. The variables are $\mathscr{D}$ for divergence, WSPD for wind speed, SST for sea surface temperature, T_+ and q_+ for temperature and humidity above the boundary layer and ΔF_R for cloud-top radiative driving; α denotes a sensitivity parameter, namely the entrainment ef cien cy. Note that the maximum LWP for variations in $\mathscr{D}$ is 300 gm^{-1} and hence is off-scale.

thus numerical issues (such as convergence on the vertical grid) can be avoided; and (iii) it is familiar to us and has well-defined properties, including analytic solutions in certain limits (Stevens, 2005; Zhang et al., 2005).

3. A stochastically perturbed mixed-layer model

Next we explore the behavior of (1) as a function of idealized variability in the large-scale state and uncertainty in model parameters. In particular we systematically evaluate the behavior of the model by letting different large-scale parameters be represented as random variables, whose mean and variance is given by the data. To render the noise smooth for our calculations we specified the shape of the power spectral density of the variable in question to wit a log-normal spectrum with a spectral peak at 2 days. Different realizations were then could be constructed by randomizing the phases of the spectral coefficients. Because our chosen spectral density has very little power at time scales comparable to the time step used to integrate (1), this results in a smooth model of the noise.

Results of this exercise are presented in Fig. 6. They principally show the sensitivity of the boundary layer physics to the estimated uncertainty in various large-scale forcing fields, and the entrainment efficiency as measured by the parameter α. Overall the results are most sensitive to the variability of $\mathscr{D}$ in the data; uncertainty, or variability, in the structure of the free troposphere as represented by T_+ and q_+ and the entrainment efficiency α also significantly affect the results. Near 120 W and 30 N at least, variability in sea surface temperatures (SSTs), wind speeds and radiative forcing play a rather minor role in the structure of the solutions. The rather large sensitivity of the solutions to $\mathscr{D}$ might explain why large-scale motions are so visually manifest in the cloud field.

Despite the proximity to a region of parameter space which supports multiple equilibria, model (1) behaves relatively linearly. In this regime, the mean state of the model forced by the mean fields is a good representation of the mean state that would result from averaging over randomly forced states. This result is consistent with previous studies using (1), which compared the difference between the mean cloud field as represented by the

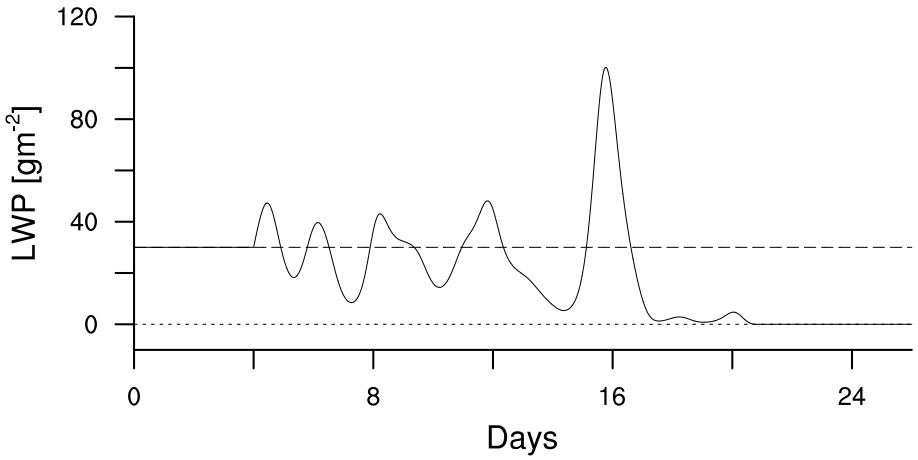

Figure 7: Illustration of the mixed-layer state transition from the cloudy regime to the clear regime, due to perturbations around a large-scale divergence value of $\mathcal{D} = 5 \times 10^{-6}\ S^{-1}$. The dashed and dotted lines are the expected LWP values for the cloudy (upper) and the clear (lower) regimes; the solid line is the transient behavior.

mean radiative forcing and the average cloud field for diurnally varying radiative forcing (Zhang et al., 2005). It also suggests that adding noise to the model physics, as a proxy for unrepresented variability, is unlikely to change the mean behavior of the IFS in this regime.

Our Fig. 6 thus suggests that the deficiencies of the boundary layer physics in the IFS are structural, and must be addressed as such. For instance, overly shallow and stratified boundary layers are consistent with the production of turbulence by radiative cooling at cloud top not being sufficiently vigorous in the IFS. On the one hand, deficiencies of this type are unlikely to be captured, or remedied, by stochastic effects; on the other hand, trying to do so can expose structural deficiencies of the model. In the latter capacity, stochastic methods can be a valuable tool in parameterization evaluation, even if they do not directly solve the "parameterization problem."

In addition to its diagnostic merits, adding noise to the system, has some further advantages. Figure 7 shows the behavior of the mixed-layer model in a region of parameter space that allows multiple equilibria. In Fig. 7, the mixed-layer system starts from the cloudy solution; when subject to a random realization of noise in the divergence field, it begins to fluctuate about its initial equilibrium; when the stochastic perturbations accumulate sufficiently to overcome the potential barrier, the mixed-layer model flips to a clear regime.

This transition, wherein the breaks of cloud deck are promoted by random disturbances of the large-scale parameters, is reminiscent of other phase transitions (Landau and Lifshitz, 1994; Anderson, 1997) in climate-related problems (Moritz and Sutera, 1981; Ghil and Childress, 1987; Miller et al., 1994). To explore further this transition, we have started to study the variability in stratocumulus cloud fraction climatology using a stochastic lattice model. We illustrate in Fig. 8 how stochastic effects affect the spatial distribution of cloudiness variables. In particular, the discrete cloud fraction in the mixed-layer model (i.e., cloudy or not) can be generalized so as to allow for partial cloudiness, thereby being rendered continuous. More interestingly, we expect nearest-neighbor interactions between columns to generate self-organized structures in the cloud deck (Xu et al., 1992; Khouider et al., 2003).

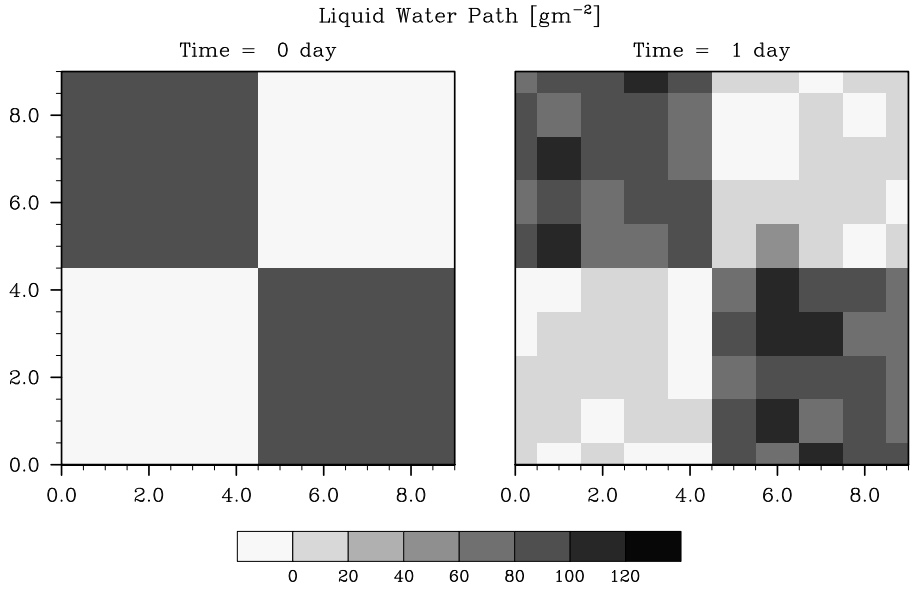

Figure 8: Illustration of the mixed-layer state transition between cloudy (LWP > 0, grey and dark areas) and clear (LWP = 0, white areas) regimes in the stochastic lattice model, due to perturbations in large-scale conditions. Left panel is the initial state; right panel is the state after one day, indicating numerous transitions at the subgrid-scale.

4. Summary and conclusions

The representation of the stratocumulus-topped boundary layer was investigated using a mixed-layer model, one month of forecasts by the IFS, the 40-year reanalysis of meteorological data by the ECMWF (ERA40), and data from a recent field study (DYCOMS-II). The comparison of ERA40 and IFS data with the observations show that, despite a relatively good prediction of the large-scale environment in the stratocumulus regions, ERA40 as well as the IFS tend to produce a boundary layer that is too stratified and too shallow; both these features are consistent with too little boundary-layer cloudiness.

The quality of the large-scale environment represented by ERA40 encourages diagnostic studies with boundary layer parameterizations to help evaluate what factors may determine the structure of the boundary layer. We performed such studies with a single-column mixed-layer model governed by a system of three ODEs that naturally couple radiative, cloud, and turbulent processes. The model was shown to represent the structure of the observed boundary layer at least as well as the IFS, given the monthly mean forcing.

A simple model of the noise was used to represent unresolved variability in large-scale fields, or uncertainty in model parameters. Adding stochastic variability in this manner shows that noise has very little effect on the predicted mean state of the model, and hence suggests that deficiencies in the IFS representation of the boundary layer are structural and need to be addressed first in a deterministic context. In addition to being a useful diagnostic tool, the incorporation of noise into the mixed-layer framework has other advantages, as it helps render formally discrete aspects of the model (i.e., cloud fraction) continuous. The addition of noise also allowed us to explore interesting implications of the multiple equilibria of the parameterized physics, thereby forcing cloud transitions that would not otherwise occur.

In summary, these results suggest that the incorporation of the effects from stochastic variability on parameterizations can provide valuable insights into their behavior, even in cases when it does not systematically change

the latter. Attempts to incorporate stochastic processes may thus significantly aid systematic parameterization development of unresolved physics by large-scale models, A fuller investigation of the lattice models touched upon here would be another important step in this direction.

Acknowledgments

This work was supported by NSF grants ATM-0336849, ATM-9985413, NASA grant NAG512559 (Bjorn Stevens and Yunyan Zhang) and NSF grant ATM00-82131 (Michael Ghil and Yunyan Zhang). Conversations with Martin Köhler on the interpretation of the ERA40 data, and the behavior of the IFS are gratefully acknowledge, as is the assistance of Martin Miller and Anton Beljaars in providing DDH data for comparison with the DYCOMS-II observations.

References

Agee, E. M., 1984: Observations from space and thermal convection: A historical perspective. *Bull. Amer. Meteor. Soc.*, **65**, 938–949.

Anderson, P. W., 1997: *Basic Notions of Condensed Matter Physics*. Perseus Publishing, 564pp.

Atkinson, B. W. and J. W. Zhang, 1996: Mesoscale shallow convection in the atmosphere. *Rev. Geophys.*, **34**, 403–431.

Charney, J. G. and J. G. DeVore, 1979: Multiple flow equilibria in the atmosphere and blocking. *J. Atmos. Sci.*, **36**, 1205–1216.

Ghil, M. and S. Childress, 1987: *Topics in Geophysical Fluid Dynamics: Atmospheric Dynamics, Dynamo Theory and Climate Dynamics*. Springer-Verlag, New York/Berlin/London/Paris/Tokyo, 485pp.

Khouider, B., A. J. Majda and M. A. Katsoulakis, 2003: Coarse-grained stochastic models for tropical convection and climate. *Proc. Natl. Acad. Sci.*, **100**, 11941–11946.

Koo, S. and M. Ghil, 2002: Successive bifurcations in a simple model of atmospheric zonal-flow vacillation. *Chaos*, **12**, 300–309.

Landau, L. D. and E. M. Lifshitz, 1994: *Statistical Physics Part I*. vol. 5 of *Course of Theoretical Physics*. Pergamon, 3rd edition, 512pp.

Lewellen, D. C. and W. Lewellen, 1998: Large-eddy boundary layer entrainment. *J. Atmos. Sci.*, **55**, 2645–2665.

Li, Z.-X., K. Ide, H. Le Treut and M. Ghil, 1997: Atmospheric radiative equilibria in a simple column model. *Clim. Dyn.*, **13**, 429–440.

Lilly, D. K., 1968: Models of cloud topped mixed layers under a strong inversion. *Quart. J. Roy. Meteor. Soc.*, **94**, 292–309.

Miller, R. N., M. Ghil and F. Gauthiez, 1994: Advanced data assimilation in strongly nonlinear dynamical systems. *J. Atmos. Sci.*, **51**, 1037–1056.

Moritz, R. E. and A. Sutera, 1981: The predictability problem – effects of stochastic perturbations in multi-equilibrium systems. *Adv. Geophys.*, **23**, 345–383.

North, G. R., R. F. Cahalan and J. A. Coakley, Jr., 1981: Energy balance climate models. *Rev. Geophys. Space Phys.*, **19**, 91–121.

Randall, D. A. and M. J. Suarez, 1984: On the dynamics of stratocumulus formation and dissipation. *J. Atmos. Sci.*, **41**, 3052–3057.

Rennó, N. O., 1997: Multiple equilibria in radiative-convective atmospheres. *Tellus*, **49A**, 423–428.

Stevens, B., 2002: Entrainment in stratocumulus mixed layers. *Quart. J. Roy. Meteor. Soc.*, **128**, 2663–2690.

Stevens, B., 2005: Bulk boundary layer concepts for simple models of tropical dynamics. *Theoret. Comput. Fluid Dynamics*, submitted.

Stevens, B., A. Beljaars, S. Bordoni, C. Holloway, M. Köhler, S. K. V. Savic-Jovcic and Y. Zhang, 2005a: On the sturcture of the lower troposphere: July 2001 near 120W and 30N. *J. Climate*, submitted.

Stevens, B., D. H. Lenschow, G. Vali, H. Gerber, A. Bandy, B. Blomquist, C. S. B. J.-L. Brenguier, F. Burnet, T. Campos, S. Chai, D. F. I. Faloona, S. Haimov, K. Laursen, D. K. Lilly, S. P. M. S. M. Loehrer, B. Morely, M. D. Petters, L. R. D. C. Rogers, V. Savic-Jovcic, J. R. Snider, D. Straub, M. J. Szumowski, H. Takagi, D. Thorton, M. Tschudi, M. W. C. Twohy, and M. C. van Zanten, 2003: DYCOMS-II. *Bull. Amer. Meteor. Soc.*, **84**, 579–593.

Stevens, B., G. Vali, K. Comstock, R. Wood, M. C. van Zanten Phil Austin, C. Bretherton, D. H. Lenschow and I. Faloona, 2005b: Pockets of open cells and drizzle in marine stratocumulus. *Bull. Amer. Meteor. Soc.*, **86**, 51–57.

Xu, K.-M., A. Arakawa and S. K. Krueger, 1992: The macroscopic behavior of cumulus ensembles simulated by a cumulus ensemble model. **49**, 2402–2420.

Zhang, Y., B. Stevens and M. Ghil, 2005: On the diurnal cycle and susceptibility to aerosol concentration in a stratocumulus-topped mixed layer. *Quart. J. Roy. Meteor. Soc.*, **131**, 1567–1584.